Dynamics of Electron Hopping in Assemblies of Redox Centers. Percolation and Diffusion

David N. Blauch and Jean-Michel Savéant*

Contribution from the Laboratoire d'Electrochimie Moléculaire de l'Université de Paris 7, Unité Associée au CNRS No. 438, 2 Place Jussieu, 75251 Paris Cedex 05, France.
Received September 17, 1991

Abstract: The interdependence of electron hopping between redox centers and the physical motion of redox centers is investigated systematically. When physical motion is either nonexistent or much slower than electron hopping, charge propagation is fundamentally a percolation process. In the opposite extreme, rapid molecular motion thoroughly rearranges the molecular distribution between successive electron hops, thereby leading to mean-field behavior. Monte-Carlo simulations are employed to study the transition between static percolation and mean-field behaviors as a function of the relative rates of electron hopping and physical motion. Previously derived mean-field equations for free physical diffusion (Dahms–Ruff) are shown to be inapplicable to systems in which the contribution of physical diffusion to charge transport is small compared to that of electron hopping. The concept of bounded diffusion, based upon a simple and approximate harmonic model, is developed and employed in the description of charge propagation in systems where the redox centers are irreversibly attached to a surrounding supramolecular structure. The mean-field limit for bounded diffusion (Laviron–Andrieux–Savéant behavior) is reached when the rate of physical motion exceeds that of electron hopping and the range of physical motion is sufficiently great to permit interactions between neighboring redox molecules. An important consequence of this analysis is that the rate constant involved in the proportionality between the apparent diffusion coefficient and the concentration of redox sites is the activation-controlled rate constant and not a combination of the diffusion- and activation-controlled rate constants. Physical motion, however, manifests itself in the mean-squared displacement of an electron between successive electron hops, which, in addition to the electron hopping distance, includes a term characterizing the distance a molecule is permitted to move by the surrounding supramolecular structure to which it is attached.

Supramolecular systems[1] containing redox moieties constitute an important field of research with applications to sensors,[2] electrocatalysis[3] and electrosynthesis,[3a] molecular electronics,[4] energy conversion,[5] and immobilization of enzymes onto electrode surfaces.[6] Research has involved both three-dimensional systems, such as redox polymers,[7] and two-dimensional systems, such as Langmuir–Blodgett[8,9] and self-assembled[10] monolayers and bilayers. A key issue in the development of supramolecular redox systems is the determination of the exact mechanism of charge transport within such systems and of the relationship between the rate of charge transport and the concentration of redox centers.[11]

The transport of electrons through macromolecular structures containing redox molecules occurs via physical displacement of the redox molecules and electron hopping from one reduced molecule to an adjacent oxidized molecule. In solution, charge transport is dominated by physical diffusion of the redox molecules. Enhancement of the charge transport rate by electron exchange is predicted to occur in solutions containing mixtures of the oxidized and reduced species as described by Dahms[12a] and Ruff et al.[12b,c] The diffusion coefficient, D_{ap}, resulting from a combination of physical displacement and electron hopping is given by[13]

$$D_{ap} = D_{phys} + k_{ex}C_E\delta^2/6 \quad (1)$$

where D_{phys} is the diffusion coefficient for physical displacement of the redox molecules, k_{ex} is the bimolecular rate constant for electron self-exchange, C_E is the total concentration of redox species, and δ is the center-to-center distance between redox centers at the time of electron transfer. The salient feature of the Dahms–Ruff equation is the expression of D_{ap} as the sum of the contributions arising from physical motion and electron exchange with the concentration dependence of D_{ap} permitting quantification of the two components.

The Dahms–Ruff equation has been widely applied to redox polymer systems in which physical diffusion is much slower than in solution and may no longer exceed the rate of electron hopping or may even be negligibly slow as compared to electron hopping.[14-20] On the other hand, Laviron[21a] and Andrieux and

(1) (a) For a general review of supramolecular chemistry, see: refs 1b–d and references cited therein. (b) Lehn, J.-M. *Angew. Chem., Int. Ed. Engl.* **1988**, *27*, 89. (c) Lehn, J.-M. *Angew. Chem., Int. Ed. Engl.* **1990**, *29*, 1304. (d) Ringsdorf, H.; Schlarb, B.; Venzmer, J. *Angew. Chem., Int. Ed. Engl.* **1988**, *27*, 113.

(2) Hable, C. T.; Crooks, R. M.; Wrighton, M. S. *J. Phys. Chem.* **1989**, *93*, 1190.

(3) (a) Rusling, J. F. *Acc. Chem. Res.* **1991**, *24*, 75. (b) Andrieux, C. P.; Savéant, J.-M. Catalysis at Redox Polymer Coated Electrodes. In *Molecular Design of Electrodes Surfaces*; Murray, R. W., Ed.; Techniques in Chemistry; Wiley: New York, in press.

(4) (a) Metzger, R. M.; Panetta, C. A. *New J. Chem.* **1991**, *15*, 209. (b) Polymeropoulos, E. E.; Möbius, D.; Kuhn, H. *Thin Solid Films* **1980**, *68*, 173. (c) Hickman, J. J.; Zou, C.; Ofer, D.; Harvey, P. D.; Wrighton, M. S.; Laibinis, P. E.; Bain, C. D.; Whitesides, G. M. *J. Am. Chem. Soc.* **1989**, *111*, 7271. (d) Lindsey, J. S. *New J. Chem.* **1991**, *15*, 153.

(5) Meyer, T. J. *Acc. Chem. Res.* **1989**, *22*, 163.

(6) Heller, A. *Acc. Chem. Res.* **1990**, *23*, 128.

(7) (a) For reviews of this field, see: refs 6b–e and references cited therein. (b) Murray, R. W. *Acc. Chem. Res.* **1980**, *13*, 135. (c) Murray, R. W. *Annu. Rev. Mater. Sci.* **1984**, *14*, 145. (d) Faulkner, L. R. *Chem. Eng. News* **1984**, *62*, 28. (e) Chidsey, C. E. D.; Murray, R. W. *Science* **1986**, *231*, 25.

(8) (a) Naito, K.; Miura, A.; Azuma, M. *Langmuir* **1991**, *7*, 627. (b) Kubota, M.; Ozaki, Y.; Araki, T.; Ohki, S.; Iriyama, K. *Langmuir* **1991**, *7*, 774. (c) Zhang, X.; Bard, A. J. *J. Am. Chem. Soc.* **1989**, *111*, 8090.

(9) (a) Charych, D. H.; Landau, E. M.; Majda, M. *J. Am. Chem. Soc.* **1991**, *113*, 3340. (b) Widrig, C. A.; Miller, C. J.; Majda, M. *J. Am. Chem. Soc.* **1988**, *110*, 2009. (c) Bourdillon, C.; Majda, M. *J. Am. Chem. Soc.* **1990**, *112*, 1795. (d) Miller, C. J.; Widrig, C. A.; Charych, D. H.; Majda, M. *J. Phys. Chem.* **1988**, *92*, 1928. (e) Goss, C. A.; Miller, C. J.; Majda, M. *J. Phys. Chem.* **1988**, *92*, 1937. (f) Miller, C. J.; Majda, M. *Anal. Chem.* **1988**, *60*, 1168. (g) Goss, C. A.; Majda, M. *J. Electroanal. Chem.* **1991**, *300*, 377.

(10) (a) Shimomura, M.; Utsugi, K.; Horikoshi, J.; Okuyama, K.; Hatozaki, O.; Oyama, N. *Langmuir* **1991**, *7*, 760. (b) Chidsey, C. E. D.; Loiacono, D. N. *Langmuir* **1990**, *6*, 682. (c) Möbius, D. *Ber. Bunsen-Ges. Phys. Chem.* **1978**, *82*, 848. (d) Swalen, J. D.; Allara, D. L.; Andrade, J. D.; Chandross, E. A.; Garoff, S.; Israelachvili, J.; McCarthy, T. J.; Murray, R.; Pease, R. F.; Rabolt, J. F.; Wynne, K. J.; Yu, H. *Langmuir* **1987**, *3*, 932.

(11) Majda. Dynamics of Electron Transport in Polymeric Assemblies of Redox Centers. In *Molecular Design of Electrodes Surfaces*; Murray, R. W., Ed.; Techniques in Chemistry; Wiley: New York, in press.

(12) (a) Dahms, H. *J. Phys. Chem.* **1968**, *72*, 362. (b) Ruff, I.; Friedrich, V. J. *J. Phys. Chem.* **1971**, *75*, 3297. (c) Ruff, I.; Friedrich, V. J.; Demeter, K.; Csaillag, K. *J. Phys. Chem.* **1971**, *75*, 3303.

(13) (a) An error in the derivation of eq 1 in ref 11b gave rise to an incorrect value ($\pi/4$) for the geometric factor. The correct value (see ref 13b–d) for three-dimensional systems is $^1/_6$. (b) Ruff, I.; Botár, L. *J. Chem. Phys.* **1985**, *83*, 1292. (c) Ruff, I.; Botár, L. *Chem. Phys. Lett.* **1986**, *126*, 348. (d) Ruff, I.; Botár, L. *Chem. Phys. Lett.* **1988**, *149*, 99.

0002-7863/92/1514-3323$03.00/0

Savéant[21b] have explicitly examined the behavior expected for redox polymer systems in which physical diffusion of the redox centers does not contribute to charge transport, because the redox centers are physically attached to the macromolecular structure (covalent or coordinative attachment or strong electrostatic binding) and have derived the relationship[21c]

$$D_{ap} = k_{ex}C_E\Delta x^2/6 \quad (2)$$

where k_{ex} and C_E have the same meaning as before. The distance Δx is defined as the thickness of a "monolayer" of redox centers, a definition that is not free of ambiguity. In the subsequent literature, eq 2 has most generally been considered as a particular limiting case of eq 1 corresponding to the absence of physical motion of the redox centers ($D_{phys} = 0$):

$$D_{ap} = k_{ex}C_E\,\delta^2/6$$

In fact, Dahms–Ruff theory describes charge transport arising from electron hopping between freely diffusion redox centers, whereas Laviron–Andrieux–Savéant theory describes charge transport arising from electron hopping between redox centers that are irreversibly attached to a supramolecular structure. They have in common the prediction of a linear variation of the apparent diffusion coefficient with the total concentration of redox centers.

In recent years, the exact nature of the phenomena that control the rate constant k_{ex} has been the subject of active discussion. It has been suggested[14c,15a,c,i,22] that the rate of electron exchange cannot exceed the rate at which reactants encounter each other; i.e., k_{ex} cannot exceed the bimolecular diffusion-limited rate constant, k_{diff}, which is related to D_{phys} by[23]

$$k_{diff} = 8\,\pi\delta D_{phys}N_A \quad (3)$$

where N_A is the Avogadro number. The appropriate value for k_{ex} is then obtained from the classical Noyes expression[24]

$$1/k_{ex} = 1/k_{act} + 1/k_{diff}$$

where k_{act} is the bimolecular activation-limited rate constant for electron self-exchange. This line of reasoning was taken further by Ruff et al.[12b] who suggested that k_{diff} is determined not by D_{phys} but by D_{ap}, meaning that the diffusion-limited rate constant itself increases with the concentration of the redox species. Another approach to the problem of charge transport in redox polymers has been to view the system as being composed of strictly immobile redox centers exchanging electrons by means of an "extended electron transfer" mechanism.[25]

As is made clear in the following sections, the main reason these approaches have not produced a satisfactory description of the charge transport mechanism is that they have ignored the percolation aspects of the problem. Charge transport arising from electron hopping between strictly immobile centers is fundamentally a percolation process. Application of the percolation concepts[26] to electron hopping between immobile redox centers leads to the following picture. The random distribution of redox centers yields a collection of clusters in which each molecule in a cluster is accessible by hops between molecules occupying adjacent sites. An electron is able to travel throughout a specific cluster but can never escape beyond the confines of that cluster. Charge transport, therefore, cannot occur across regions exceeding the size of the largest cluster. Below a critical concentration (the percolation threshold), all clusters are of finite, microscopic size; thus charge transport across macroscopic distances is impossible. Above the percolation threshold, a dominant cluster (the percolation cluster) spans the entire system, regardless of the system dimensions, making charge transport across macroscopic distances possible.

When the redox centers are able to freely diffuse, the clusters within the system are constantly changing and reorganizing, resulting in percolation of electrons on a dynamic distribution of molecules. General analyses of dynamic percolation involving random renewal of the hopping probabilities have been developed in recent years.[27,28] The theory has been applied to ionic charge transport in oil–water emulsions[27a,29] and solid polymer electrolytes.[28b-e] In the present case of electron hopping between redox centers, as the rate of physical motion increases relative to that of electron hopping, the microscopic distribution of redox centers eventually reorganizes sufficiently rapidly and thoroughly to eliminate any correlation between the geometry of the clusters existing during successive electron hops. In this limit, the mean-field approximation is valid and the Dahms–Ruff equation, originally derived for conditions where physical diffusion is much

(14) (a) Oyama, N.; Anson, F. C. *J. Electroanal. Chem.* **1980**, *127*, 640. (b) Buttry, D. A.; Anson, F. C. *J. Electroanal. Chem.* **1981**, *130*, 333. (c) Buttry, D. A.; Anson, F. C. *J. Am. Chem. Soc.* **1983**, *105*, 685. (d) Anson, F. C.; Blauch, D. N.; Savéant, J.-M.; Shu, C.-F. *J. Am. Chem. Soc.* **1991**, *113*, 1922. (e) Shigehara, K.; Oyama, N.; Anson, F. C. *J. Am. Chem. Soc.* **1981**, *103*, 2552. (f) Anson, F. C.; Savéant, J.-M.; Shigehara, K. *J. Am. Chem. Soc.* **1983**, *105*, 1096. (g) Buttry, D. A.; Savéant, J.-M.; Anson, F. C. *J. Phys. Chem.* **1984**, *88*, 3086. (h) Anson, F. C.; Ohsaka, T.; Savéant, J.-M. *J. Phys. Chem.* **1983**, *87*, 640. (i) Oyama, N.; Yamaguchi, S.; Nishiki, Y.; Tokuda, K.; Matsuda, H.; Anson, F. C. *J. Electroanal. Chem.* **1982**, *139*, 371.

(15) (a) Surridge, N. A.; Jernigan, J. C.; Dalton, E. F.; Buck, R. P.; Watanabe, M.; Zhang, H.; Pinkerton, M.; Wooster, T. T.; Longmire, M. L.; Facci, J. S.; Murray, R. W. *Faraday Discuss. Chem. Soc.* **1989**, *88*, 1. (b) Jernigan, J. C.; Surridge, N. A.; Zvanut, M. E.; Silver, M.; Murray, R. W. *J. Phys. Chem.* **1989**, *93*, 4620. (c) Geng, L.; Reed, R. A.; Kim, M.-H.; Wooster, T. T.; Oliver, B. N.; Egekeze, J.; Kennedy, R. T.; Jorgenson, J. W.; Parcher, J. F.; Murray, R. W. *J. Am. Chem. Soc.* **1989**, *111*, 1614. (d) Dalton, E. F.; Surridge, N. A.; Jernigan, J. C.; Wilbourn, K. O.; Facci, J. S.; Murray, R. W. *Chem. Phys.* **1990**, *141*, 143. (e) Watanabe, M.; Wooster, T. T.; Murray, R. W. *J. Phys. Chem.* **1991**, *95*, 4573. (f) Geng, L.; Reed, R. A.; Longmire, M.; Murray, R. W. *J. Phys. Chem.* **1987**, *91*, 2908. (g) Watanabe, M.; Longmire, M. L.; Murray, R. W. *J. Phys. Chem.* **1990**, *94*, 2614. (h) Facci, J. S.; Schmehl, R. H.; Murray, R. W. *J. Am. Chem. Soc.* **1982**, *104*, 4959. (i) Daum, P.; Lenhard, J. R.; Rolison, D.; Murray, R. W. *J. Am. Chem. Soc.* **1980**, *112*, 4649. (j) Jernigan, J. C.; Murray, R. W. *J. Am. Chem. Soc.* **1987**, *109*, 1738. (k) Daum, P.; Murray, R. W. *J. Phys. Chem.* **1981**, *85*, 389. (l) Jernigan, J. C.; Murray, R. W. *J. Phys. Chem.* **1987**, *91*, 2030. (m) Facci, J.; Murray, R. W. *J. Electroanal. Chem.* **1981**, *124*, 339. (n) Nakahama, S.; Murray, R. W. *J. Electroanal. Chem.* **1983**, *158*, 303. (o) Schmehl, R. H.; Murray, R. W. *J. Electroanal. Chem.* **1983**, *152*, 97.

(16) (a) Oh, S. M.; Faulkner, L. R. *J. Electroanal. Chem.* **1989**, *269*, 77. (b) Majda, M.; Faulkner, L. R. *J. Electroanal. Chem.* **1984**, *169*, 77. (c) Chen, X.; He, P.; Faulkner, L. R. *J. Electroanal. Chem.* **1987**, *222*, 223.

(17) (a) Doblhofer, K.; Lange, R. *J. Electroanal. Chem.* **1987**, *229*, 239. (b) Doblhofer, K.; Braun, H.; Lange, R. *J. Electroanal. Chem.* **1986**, *206*, 93. (c) Lange, R.; Doblhofer, K. *J. Electroanal. Chem.* **1987**, *216*, 241.

(18) (a) White, H. S.; Leddy, J.; Bard, A. J. *J. Am. Chem. Soc.* **1982**, *104*, 4811. (b) Martin, C. R.; Rubinstein, I.; Bard, A. J. *J. Am. Chem. Soc.* **1982**, *104*, 4817.

(19) (a) Whiteley, L. D.; Martin, C. R. *J. Phys. Chem.* **1989**, *93*, 4650. (b) Martin, C. R.; Dollard, K. A. *J. Electroanal. Chem.* **1983**, *159*, 127.

(20) (a) He, P.; Chen, X. *J. Electroanal. Chem.* **1988**, *256*, 353. (b) Chambers, J. Q.; Kaufman, F. B.; Nichols, K. H. *J. Electroanal. Chem.* **1982**, *142*, 277. (c) Schroeder, A. H.; Kaufman, F. B.; Patel, V.; Engler, E. M. *J. Electroanal. Chem.* **1980**, *113*, 193. (d) Elliott, C. M.; Redepennig, J. G. *J. Electroanal. Chem.* **1984**, *181*, 137. (e) Sharp, M.; Lindholm, B.; Lind, E. L. *J. Electroanal. Chem.* **1989**, *274*, 35. (f) Rubinstein, I. *J. Electroanal. Chem.* **1985**, *188*, 227.

(21) (a) Laviron, E. *J. Electroanal. Chem.* **1980**, *112*, 1. (b) Andrieux, C. P.; Savéant, J.-M. *J. Electroanal. Chem.* **1980**, *111*, 377. (c) The factor $^1/_6$ was lacking in the original derivation, because k_{ex} was represented as the rate constant for electron exchange between two nearest-neighbor molecules rather than the usual bimolecular rate constant (see ref 14d).

(22) See, however, refs 14d and 15e, where k_{ex} is regarded as being inherently equal to k_{act}.

(23) (a) von Smoluchowski, M. *Phys. Z.* **1916**, *17*, 557. (b) von Smoluchowski, M. *Phys. Z.* **1916**, *17*, 583. (c) Moore, J. W.; Pearson, R. G. *Kinetics and Mechanism*, 3rd ed.; Wiley: New York, 1981; Chapter 7.

(24) (a) The Noyes expression[24b] is used in a manner analogous to that for electron-transfer reactions in solution. See: ref 24c and references cited therein. (b) Noyes, R. M. *J. Chem. Phys.* **1954**, *22*, 1349. (c) Sutin, N. *Acc. Chem. Res.* **1982**, *15*, 275.

(25) Fritsch-Faules, I.; Faulkner, L. R. *J. Electroanal. Chem.* **1989**, *263*, 237.

(26) (a) Broadbent, S. R.; Hammersley, J. M. *Proc. Cambridge Phil. Soc.* **1957**, *53*, 629. (b) Shante, V. K. S.; Kirkpatrick, S. *Adv. Phys.* **1971**, *20*, 325. (c) Kirkpatrick, S. *Rev. Mod. Phys.* **1973**, *45*, 574. (d) Zallen, R. *The Physics of Amorphous Solids*; Wiley: New York, 1983; Chapter 4.

(27) (a) Grest, G. S.; Webman, I.; Safran, S. A.; Bug, A. L. R. *Phys. Rev. A* **1986**, *33*, 2842. (b) Bug, A. L. R.; Gefen, Y. *Phys. Rev. A* **1987**, *35*, 1301.

(28) (a) Druger, S. D.; Nitzan, A.; Ratner, M. A. *J. Chem. Phys.* **1983**, *79*, 3133. (b) Druger, S. D.; Ratner, M. A.; Nitzan, A. *Phys. Rev. B* **1985**, *31*, 3939. (c) Ratner, M. A.; Nitzan, A. *Faraday Discuss. Chem. Soc.* **1989**, *88*, 19. (d) Granek, R.; Nitzan, A. *J. Chem. Phys.* **1989**, *90*, 3784. (e) Granek, R.; Nitzan, A.; Druger, S. D.; Ratner, M. A. *Solid State Ionics* **1988**, *28–30*, 128. (f) Druger, S. D.; Ratner, M. A.; Nitzan, A. *Mol. Cryst. Liq. Cryst.* **1990**, *190*, 171.

(29) Ponton, A.; Bose, T. K.; Delbos, G. *J. Chem. Phys.* **1991**, *94*, 6879.

faster than electron exchange, should apply.

In the following sections, we describe a Monte-Carlo simulation technique that we have employed to study the transition between static percolation and mean-field behavior. Our simulations involving free physical diffusion of the redox centers enable us to define the conditions under which the mean-field approximation is applicable. An important consequence of this analysis is that the Dahms–Ruff equation is inherently unable to describe the charge transport mechanism in systems where the physical motion of the redox centers is so slow or so restricted in range as to contribute negligibly to the overall conduction. This limitation is particularly true for systems in which the redox centers are irreversibly attached to the macromolecular structure but are not strictly immobile. Physical displacement of the redox centers around the anchoring points, i.e., "bounded diffusion", is possible, but such motion is obviously too restricted in scope to contribute directly to charge transport. Examples of such systems exist, with D_{ap} being observed to increase with the concentration of redox centers and to approach zero as the concentration of redox centers approaches zero.[14d,15b,20e] These observations are consistent with the Laviron–Andrieux–Savéant equation, suggesting that this equation could serve as a basis for describing charge transport in systems containing irreversibly attached redox centers under mean-field conditions. In this case, as in the case for free diffusion, the question arises as to the possible ability of bounded diffusion to reorganize the percolation clusters sufficiently rapidly and extensively to achieve mean-field conditions. We have developed in this connection a simple and approximate model of bounded diffusion of the redox centers, which, when sufficiently rapid and extensive, ensures the establishment of mean-field conditions while the direct contribution of physical motion to the rate of charge transport remains negligible. In this limit, we have found that D_{ap} is given by eq 2 with $k_{ex} = k_{act}$; however, Δx^2 is not equal to δ^2 but rather to $\delta^2 + 3\lambda^2$, in the three-dimensional case, and to $\delta^2 + 2\lambda^2$, in the two-dimensional case, where λ characterizes the mean displacement of a redox molecule out of its equilibrium position. This same bounded-diffusion model was then incorporated into Monte-Carlo simulations in order to describe the transition between static percolation and mean-field conditions as the rate and range of bounded diffusion increase relative to that of electron hopping.

In the analyses below we have disregarded influences arising from the solvent, spectator ions, and the supramolecular structure. While the effects associated with these components are undoubtedly important, they are secondary to the objectives of our study, which are to establish the fundamental laws of charge transport arising from electron hopping in assemblies of redox centers and to discuss the validity or lack thereof of mean-field approximations that have been previously used to describe such processes. In view of the recent development of two-dimensional assemblies of redox molecules, the results will be presented for both two- and three-dimensional systems.

Results and Discussion

Simulation Model. In this investigation the redox system is modeled as a square (two dimensions) or simple cubic (three dimensions) lattice. The lattice is a small, but macroscopic, portion of the whole supramolecular system. The lattice comprises N_x, N_y, and N_z sites along the x-, y-, and z-axes, respectively, with redox molecules distributed randomly among the lattice sites. The distance, δ, between adjacent lattice sites is, in the framework of a hard sphere representation, the center-to-center distance of closest approach between two molecules; δ is thus comparable to or slightly larger than the molecular diameter. Electron exchange is assumed to occur exclusively between molecules occupying adjacent lattice sites. The fractional loading, X, is the ratio of the total number of molecules, N_E, to the total number of lattice sites, N_T. The total concentration of lattice sites is $C_T = 1/(N_A\delta^\nu)$, where ν is the dimensionality, 2 or 3, of the system.

Electron hopping between adjacent redox centers can be modeled as a Poisson process with a time constant t_e representing the average time between attempted electron hops; t_e is related to the activation-limited bimolecular rate constant according to

$$k_{act} = 1/(t_e C_T)$$

The rate of electron hopping may also be characterized by an electron hopping diffusion coefficient

$$D_e = \delta^2/(2\nu t_e) = k_{act} C_T \delta^2/(2\nu) \quad (4)$$

which is a constant representing the electron-hopping diffusion coefficient for a single electron in a system at full fractional loading. At full fractional loading, the redox molecules cannot physically move, because there are no empty sites they can reach; therefore charge transport occurs solely by electron hopping, and $D_{ap} = D_e$ at $X = 1$.

The rate at which a given electron hops between molecules is the frequency of attempted electron hops multiplied by the probability that the destination site is occupied by a molecule, which is $(1/t_e)X = (1/t_e)(C_E/C_T)$. The bimolecular rate constant k_{act} is therefore $1/(t_e C_T)$ with the corresponding pseudo-first-order rate constant being $k_{act}C_E$.

In a manner analogous to that for electron hopping, the rate of physical displacement is characterized by a time constant t_p representing the average time between attempted molecular hops in the absence of a potential energy gradient. The rate of physical motion of the redox molecules may also be characterized by a diffusion coefficient

$$D_{phys} = \delta^2/(2\nu t_p) \quad (5)$$

The conventional bimolecular diffusion-limited rate constant is related to t_p by[30]

$$k_{diff} = 4\nu\delta^{\nu-2} D_{phys} N_A = 2/(t_p C_T) \quad (6)$$

In the case of free physical diffusion of the redox molecules, D_{phys} represents the contribution of physical motion to D_{ap} at infinitely low fractional loadings ($X \rightarrow 0$) where the "blocking effects", discussed later, are absent. In a large number of redox systems of practical interest, however, diffusion of the redox molecules is not free in the sense that the molecules are attached irreversibly to the supramolecular structure. An approximate and simple model of such situations consists in regarding each redox molecule as attached to its own individual equilibrium lattice site (x_0, y_0, z_0) by an imaginary spring of force constant f_s.[31] A molecule's potential energy, ϵ, is therefore

$$\epsilon = (f_s/2)[(x - x_0)^2 + (y - y_0)^2 + (z - z_0)^2] \quad (7)$$

The probability, P_{ij}, of an attempted molecular jump from site i to adjacent site j during a time interval, Δt, is[32]

$$P_{ij} = \frac{1}{2\nu}\left(\frac{\Delta t}{t_p}\right) \exp\left(-\frac{\epsilon_j - \epsilon_i}{2k_B T}\right) \quad (8)$$

where k_B is the Boltzmann constant, T is the absolute temperature, and ϵ_i and ϵ_j are the molecule's potential energies at sites i and j, respectively. P_{ij} applies to motion to a *specific* adjacent site; the probability, P_i, of attempted motion from site i to *any* adjacent site is the sum of the probabilities for motion to all adjacent sites:

$$P_i = \sum_{j=1}^{2\nu} P_{ij} \quad (9)$$

P_{ij} can also be expressed as

$$P_{ij} = (1/2\nu)(\Delta t/t_p) \exp[-[((x_j - x_0)^2 + (y_j - y_0)^2 + (z_j - z_0)^2 - (x_i - x_0)^2 - (y_i - y_0)^2 - (z_i - z_0)^2)/2\lambda^2]]$$

introducing

$$\lambda = (2k_B T/f_s)^{1/2}$$

(30) The difference between the factor $8\pi\delta$ in eq 3 and $4\nu\delta^{\nu-2}$ in eq 6 arises from the difference in geometries. Equation 3 corresponds to spherical geometry, whereas eq 6 applies to square ($\nu = 2$) or cubic ($\nu = 3$) geometry.

(31) (a) The harmonic restriction of diffusive motion has been discussed and analyzed in ref 31b,c. (b) Chandrasekhar, S. *Rev. Mod. Phys.* **1943**, *15*, 1. (c) Agmon, N.; Hopfield, J. J. *J. Chem. Phys.* **1983**, *78*, 6947; erratum **1984**, *80*, 592.

(32) Equation 8 is a linear free energy relation with a symmetry factor of $^1/_2$.

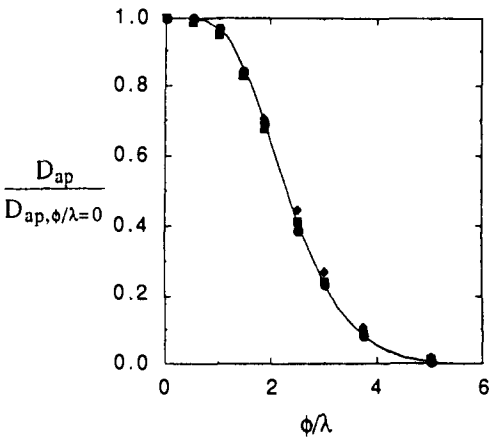

Figure 1. Variation of D_{ap}/D_{phys} with ϕ/λ in the absence of electron hopping for the simple cubic lattice. The solid line is the function $I(\phi/\lambda)$ (eq 27) with $\phi = (N_x - 1)\delta$. The points are the results of simulations for $x = 0.0625$ (●), 0.250 (■), and 0.750 (♦).

which characterizes the range of molecular motion permitted by the imaginary spring. The physical motion of the redox molecules is thus governed by two parameters, t_p and λ (or f_s). The former characterizes the time constant of the motion and the latter the spatial limitation of the motion of a redox molecule away from its equilibrium position attributable to the attachment to the macromolecular structure.

Formally, there is a continuum of situations between conditions of bounded diffusion, where the direct contribution of physical motion to charge transport is negligible because the distance λ is small compared to the total size of the system, and free diffusion ($f_s = 0$), where the contribution of physical motion to charge transport is equal to D_{phys} (eq 5). In order to describe the transition between these two limiting situtations we investigate the flux of electrons (including the electrons transported by physical displacement of the reduced molecules) through a macromolecular film of thickness ϕ perpendicular to its faces (designated as the x-coordinate) in the case where electron hopping does not contribute to charge transport. The electron flux across the film is given by Fick's first law:

$$J_e = D_{ap}\frac{dC_B}{dx} = -D_{ap}\frac{dC_A}{dx}$$

where C_B is the concentration of the reduced form of the redox couple A/B and C_A is the concentration of the oxidized form. The flux of electrons, J_e, is a function of the parameter ϕ/λ. When $\phi/\lambda \to 0$, D_{ap} approaches the apparent diffusion coefficient for free diffusion for that particular fractional loading, whereas when $\phi/\lambda \to \infty$, D_{ap} approaches zero. As shown in Figure 1, the transition between the two limiting situations occurs over a small range of values for ϕ/λ (see the Appendix for the establishment of the analytical function that relates the ratio $D_{ap}/D_{ap,\phi/\lambda=0}$ to the parameter ϕ/λ).

From inspection of Figure 1, it appears that in most cases the actual behavior of macromolecular motions will fall into one of the two limiting behaviors discussed above. These limiting behaviors, denoted as "free diffusion" and "bounded diffusion", will be successively introduced into the simulations of the transition between static percolation and mean-field conditions with no attempt to introduce the intermediate behavior depicted in Figure 1. Another reason for this simplification is that, in practice, most of the macromolecular systems will fall into one of the two limiting categories according to the presence or absence of an irreversible bonding between the redox centers and the supramolecular structure.

Returning to situations where electron hopping contributes to charge transport, the transition between static percolation and mean-field behavior was simulated by means of a Monte-Carlo procedure. During a simulation, a concentration gradient is established along the x-coordinate by reducing all oxidized molecules (A) reaching $x = 0$ and oxidizing all reduced molecules reaching $x = (N_x - 1)\delta$. The flux of electrons, J_e, across the lattice is the average of the number of electrons introduced at $x = 0$ and removed at $x = (N_x - 1)\delta$ per unit time. The apparent diffusion coefficient D_{ap} is obtained from

$$D_{ap} = \frac{J_e}{(dC_B/dx)} \tag{10}$$

Time is normalized by the time constant for electron hopping, t_e. The time constant for physical motion, t_p, is introduced as a dimensionless parameter, t_e/t_p. A simulation consists of a series of dimensionless time intervals of duration $\Delta\tau$ during which the molecules and electrons are allowed to move at random. The probability of an electron attempting to hop to an adjacent molecule during a simulation time interval is $\Delta\tau$.[33] When an electron attempts to hop, an adjacent lattice site is randomly chosen as the destination site. If the destination site is occupied by an oxidized molecule, the electron is moved; otherwise the electron hop does not occur.

In a similar manner, the probability of a freely diffusing molecule attempting to hop to an adjacent lattice site during a simulation time interval is $(t_e/t_p)\Delta\tau$.[33] In the case of bounded diffusion, this probability is P_i as defined by eq 9 with $\Delta t/t_p$ replaced by $(t_e/t_p)\Delta\tau$. When a molecule attempts to move, an adjacent site is randomly chosen as the destination site (for bounded diffusion, the probability of site j being the destination site is $P_{ij}/P_{i\cdot}$). If the destination site is unoccupied, the molecule is moved; otherwise the molecular displacement does not occur. Technical details concerning the simulations are given in the Appendix. Known limiting behaviors were simulated in order to test the integrity and precision of the simulation technique. One such behavior is the static percolation expected when the molecules are completely immobile ($t_e/t_p = 0$ or, equivalently, $D_{phys}/D_e = 0$). Our simulations yield variations of D_{ap} vs X consistent with static percolation behavior,[26] as evidenced by the dashed lines in Figure 2. Published static percolation expressions[26] concern transport of electrons under an electric field rather than under a concentration gradient. The conductivity, σ, of percolating electrons is related to the apparent diffusion coefficient by the general linear-response expression[28b,34]

$$\sigma(X) = Ne^2D_{ap}/(k_BT)$$

where N is the number of charge carriers (i.e., the number of electrons in the percolation cluster) and e is the electron charge. At full fractional loading $N = N_T$ and $D_{ap} = D_e$, thus

$$\frac{D_{ap}}{D_e} = \left(\frac{\sigma(X)}{\sigma(1)}\right)\frac{N_T}{N} = \left(\frac{\sigma(X)}{\sigma(1)}\right)\frac{1}{P(X)}$$

where $P(X)$ is the percolation probability.

In the transition from static percolation to mean-field conditions, which is dynamic percolation, the random walk of electrons between moving molecules also leads to an apparent diffusion coefficient that was computed using Fick's first law. The value of D_{ap} should be independent of the magnitude of the concentration gradient employed in the simulations; simulations employing various concentration gradients have verified this expectation.

Free Diffusion and Electron Hopping. Figure 2 depicts the variation of the apparent diffusion coefficient with the fractional loading of redox molecules for increasing values of t_e/t_p (= D_{phys}/D_e). As anticipated, the increase in the rate of physical motion as compared to that of electron hopping progressively "washes out" the critical behavior observed for static percolation; i.e., $D_{ap} = 0$ below the percolation threshold, an abrupt onset of

(33) This probability derives from Poisson statistics (see refs 35a and 36b) and is rigorously correct only when $\Delta\tau$ is substantially less than unity. In practice, we have found $\Delta\tau = 0.25$ to be sufficiently small to reduce the errors to acceptably low levels (roughly 2–3%). Values of $\Delta\tau$ were chosen to be as large as possible to keep computational times to a minimum. The same considerations also apply to the probability $(t_e/t_p)\Delta\tau$.

(34) (a) Scher, H.; Lax, M. *Phys. Rev. B* **1973**, *7*, 4491. (b) Lax, M. *Phys. Res.* **1958**, *109*, 1921. (c) Lax, M. *Rev. Mod. Phys.* **1960**, *32*, 25.

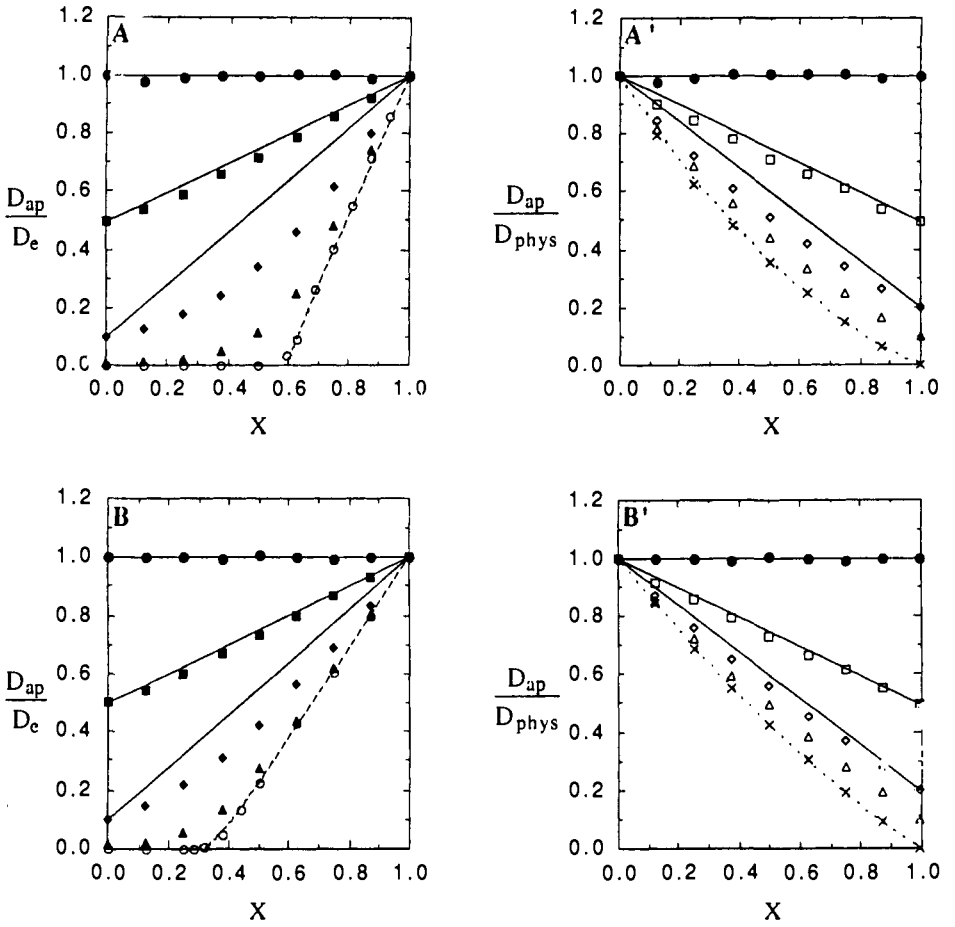

Figure 2. Variation of D_{ap}/D_e (A, B) or D_{ap}/D_{phys} (A′, B′) with x for square (A, A′) and simple cubic (B, B′) lattices for free diffusion. Points are simulation results for $t_e/t_p = 0$ (○), 0.01 (▲), 0.1 (♦), 0.5 (■), 1.0 (●), 2.0 (□), 5 (◇), 10 (△), and ∞ (×). The dashed lines represent static percolation behavior (vide supra). The dotted lines represent mean-field behavior with f_c given by eq 17. The solid lines represent mean-field behavior with $f_c = 1$.

conduction at the critical fractional loading, and a linear variation of D_{ap} with X reaching D_e at $X = 1$, as represented by the dashed line in Figure 2. The solid lines represent the variation expected on the basis of the mean-field approximation according to the following treatment.

To compute the mean-field expression for the apparent diffusion coefficient, we start with the general random walk formula:[35a,36b]

$$D_{ap} = f\langle \mathbf{r}^\bullet\, \mathbf{r}\rangle/(2\nu) \qquad (11)$$

where f is the frequency of random jumps and $\langle \mathbf{r}^\bullet\, \mathbf{r}\rangle$ is the mean-squared displacement of each jump. To proceed, we consider the frequency of random jumps to be equal to the frequency of electron hops, which is $f = X/t_e$. The vectorial displacement, $\mathbf{r}$, of an electron between two successive electron hops can be regarded as the sum of the vectorial displacement, $\mathbf{r}_e$, of the electron resulting from the electron hop and the vectorial displacement, $\mathbf{r}_p$, of the host molecule between electron hops. Assuming the electron hops and physical hops are uncorrelated,

$$\langle \mathbf{r}^\bullet\, \mathbf{r}\rangle = \langle \mathbf{r}_e^\bullet\, \mathbf{r}_e\rangle + \langle \mathbf{r}_p^\bullet\, \mathbf{r}_p\rangle \qquad (12)$$

because electron hops always occur over a distance δ, $\langle \mathbf{r}_e^\bullet\, \mathbf{r}_e\rangle = \delta^2$.

On the other hand, the mean-squared displacement of a freely diffusing molecule during a period of time t is

$$\langle \mathbf{r}_p^\bullet\, \mathbf{r}_p\rangle_t = (1 - X)f_c\delta^2(t/t_p) = 2\nu D_{phys}(1 - X)f_c + 2\nu \qquad (13)$$

where the blocking factor $(1 - X)$ accounts for the reduction in the frequency of molecular displacements attributable to obstruction by other molecules. An attempted molecular displacement is successful only if the destination site is unoccupied, the probability of which is, on average, $1 - X$; hence the effective hopping frequency is $(1 - X)/t_p$ instead of $1/t_p$. At full fractional loading ($X = 1$) no physical motion occurs, because there are no unoccupied lattice sites into which a molecule can move.

The obstruction of molecular motion by other molecules gives rise to correlation effects, accounted for by the correlation factor f_c, for which the blocking term does not account, the most important effect being the increased tendency for a molecule to return to the site it most recently vacated. If a molecule has just moved from site i to site j, site i is more likely to be unoccupied than the other sites adjacent to site j; therefore, attempted movement back to site i is more likely to be successful than attempted movement to other sites. This tendency to backtrack reduces the overall distance traveled by the molecule, leading to an observed diffusion coefficient less than that predicted by $D_{phys}(1 - X)$. The origin and implications of correlation effects (in the absence of electron hopping) have been investigated in detail.[35-37]

In order to calculate the correct value for $\langle \mathbf{r}_p^\bullet\, \mathbf{r}_p\rangle$, it is necessary to determine the distribution of times, t, between successive electron hops. The waiting time between electron hops is governed by Poisson statistics,[35a] with the probability that an electron waits a time t between successive electron hops being $(X/t_e)\exp(-Xt/t_e)$

(35) (a) Kehr, K. W.; Kutner, R.; Binder, K. *Phys. Rev. B* **1981**, *23*, 4931. (b) Kutner, R.; Kehr, K. W. *Philos. Mag. A* **1983**, *48*, 199.

(36) (a) Le Claire, A. D. In *Physical Chemistry-An Advanced Treatise*; Jost, W., Ed.; Academic Press: New York, 1970; Vol. 10, Chapter 5. (b) Kehr, K. W.; Binder, K. In *Topics in Current Physics: Applications of the Monte Carlo Method in Statistical Physics*, 2nd ed.; Binder, K., Ed.; Springer-Verlag: New York, 1987; Vol. 36, Chapter 6.

(37) (a) Fedders, P. A.; Sankey, O. F. *Phys. Rev. B* **1978**, *18*, 18. (b) Murch, G. E.; Thorn, R. J. *Philos. Mag. A* **1979**, *39*, 673. (c) Nakazato, K.; Kitahara, K. *Prog. Theor. Phys.* **1980**, *64*, 2261. (d) Koiwa, M.; Ishioka, S. *J. Stat. Phys.* **1983**, *30*, 477. (e) De Bruin, H. J.; Murch, G. E. *Philos. Mag.* **1973**, *27*, 1475. (f) Murch, G. E.; Thorn, R. J. *J. Phys. Chem. Solids* **1977**, *38*, 789.

dt. The properly weighted mean-squared physical displacement between electron hops is therefore

$$\langle \mathbf{r}_p^\circ \mathbf{r}_p \rangle = \int_0^\infty \frac{X}{t_e} \exp\left(-\frac{Xt}{t_e}\right) \langle \mathbf{r}_p^\circ \mathbf{r}_p \rangle_t \, dt \qquad (14)$$

integration of which yields

$$\langle \mathbf{r}_p^\circ \mathbf{r}_p \rangle = \left(\frac{1-X}{X}\right) f_c \delta^2 \left(\frac{t_e}{t_p}\right) \qquad (15)$$

It follows from eqs 11, 12, and 15 that

$$D_{ap} = D_{phys}(1-X)f_c + D_e X \qquad (16)$$

showing that the mean-field approximation leads to Dahms–Ruff-type behavior in which the blocking of physical diffusion is accounted for[13b-d] by the factor $1 - X$ in the first term. The correlation factor, f_c, does not appear in previous derivations.[13b-d] The value of the correlation factor has been derived in previous studies[37c] for the case where $t_e/t_p \to \infty$ ($D_e = 0$):

$$f_c = \frac{(2-X)f_{c,X=1}}{2f_{c,X=1} + (1-2f_{c,X=1})X} \qquad (17)$$

where the correlation factor at full fractional loading, $f_{c,X=1}$, is 0.466 942 and 0.653 109 for the square and simple cubic lattices, respectively.[37b,d] The predictions of Dahms–Ruff behavior (eq 16) with $D_e = 0$ and f_c given by eq 17 are represented by the dotted lines in Figure 2.

The simulations reveal that correlation effects vanish as the rate of electron hopping approaches that of physical displacement. For $t_e/t_p = 2$, the simulated values of $D_{ap}/D_{ap,X=0}$ coincide fairly closely with the mean-field values using $f_c = 1$. We have not undertaken a detailed analysis of the correlation effects observed for various values of t_e/t_p, but we can offer a qualitative explanation of the observed behavior. The correlation effects associated with physical displacement are attributable to the fact that a molecule is more likely to return to the site it most recently vacated than to move to any other adjacent site. The tendency to backtrack occurs because the site just vacated by the molecule has an above-average chance of being unoccupied. For this same reason, electron hops to the site just vacated by the molecule are *less* likely to occur than hops to other adjacent sites, because the site just vacated has a below-average change of being occupied by an oxidized molecule. The simulations suggest that when $t_e = t_p$, these two effects exactly cancel and $f_c = 1$.

The simulation results shown in Figure 2 clearly show that mean-field behavior is reached only when D_{phys} is at least as large as D_e. Whenever physical diffusion is slower than electron hopping, percolation effects are observed. These findings have an important consequence for systems in which the physical motion is so slow as to contribute insignificantly to charge transport ($D_{phys} \ll D_e$). In such cases, the variation of D_{ap} with X is expected to display static percolation behavior instead of the commonly anticipated linear variation passing through the origin. We therefore conclude that the Dahms–Ruff approach is unsuitable for the description of charge transport by means of electron hopping in systems where the redox centers are irreversibly attached to the supramolecular structure. It is also interesting to note, in the framework of the present model, that Dahms–Ruff behavior, when effectively reached, leads to a descending (or at best horizontal) variation of the apparent diffusion coefficient with the fractional loading and not to the commonly expected ascending variation.

Bounded Diffusion and Electron Hopping. As discussed above, the concept of bounded diffusion is better suited than that of free diffusion for the mean-field description of charge transport in systems where the redox centers are irreversibly attached to the supramolecular structure. Simulation data for bounded diffusion are shown in Figure 3. The variation of the apparent diffusion coefficient with the fractional loading depends upon two parameters instead of one, as in the preceding case. One parameter is again t_e/t_p ($=D_{phys}/D_e$), which compares the rates of electron hopping and physical displacement. The other is λ/δ, which compares the range of molecular motion permitted to the attached redox center by the supramolecular structure to the electron hopping distance. Whenever one of these two parameters is small, percolation effects are observed, static percolation behavior being reached asymptotically as either approaches zero (Figure 3).

Mean-field behavior is expected when both parameters become large, i.e., when the rate and range of physical displacement are sufficiently large to completely scramble the molecular clusters between successive electron hops, thereby eliminating all trace of percolation behavior. For establishing the mean-field variation of D_{ap} with X, we follow an approach similar to that employed above for the case of free diffusion. We start from eqs 11 and 12, but the expression for $\langle \mathbf{r}_p^\circ \mathbf{r}_p \rangle_t$ is now different from eq 13, because restriction of the physical motion leads to a statistical limit to how far the electron can be carried by a molecule. Extending the one-dimensional treatment of Chandrasekhar[31b,38] to two and three dimensions yields the following expression for $\langle \mathbf{r}_p^\circ \mathbf{r}_p \rangle_t$:

$$\langle \mathbf{r}_p^\circ \mathbf{r}_p \rangle_t = \langle \mathbf{r}_p^\circ \mathbf{r}_p \rangle_\infty \left[1 - \exp\left(-\frac{(1-X)f_c\delta^2 t}{\langle \mathbf{r}_p^\circ \mathbf{r}_p \rangle_\infty t_p}\right)\right] \qquad (18)$$

where the limiting mean-squared displacement, $\langle \mathbf{r}_p^\circ \mathbf{r}_p \rangle_\infty$, is $\nu\lambda^2$.

It should be noted that the treatment of Chandrasekhar does not address blocking or correlation effects; we have accounted for these effects by replacing the diffusion coefficient in Chandrasekhar's formula with $D_{phys}(1-X)f_c$. Although the blocking factor should provide an accurate correction for the actual frequency of physical jumps, it is unlikely that the f_c derived by Nakazato and Kitahara[37c] is exactly applicable to restricted diffusion. Figure 4 compares simulated values[39] of $\langle \mathbf{r}_p^\circ \mathbf{r}_p \rangle_t$ with the predictions of eq 18. For relatively low fractional loadings where correlation effects are rather minor, there is excellent agreement between the simulations and eq 18. At high fractional loadings where correlation effects are more important, small discrepancies exist between the simulated and theoretical values.

Integration of eq 21 using $\langle \mathbf{r}_p^\circ \mathbf{r}_p \rangle_t$ as defined in eq 25 yields

$$\langle \mathbf{r}_p^\circ \mathbf{r}_p \rangle = \nu\lambda^2\rho/(1+\rho) \qquad (19)$$

where ρ is the ratio of the mean-squared displacement for free diffusion after a time t_e/X (the average time between electron hops) to the maximum mean-squared displacement,

$$\rho = \left(\frac{1-X}{X}\right)\left(\frac{f_c\delta^2}{\nu\lambda^2}\right)\left(\frac{t_e}{t_p}\right) \qquad (20)$$

Combining eqs 11 and 19 with $f = X/t_e$ yields a general formula

$$D_{ap} = D_e X \qquad (21)$$

where the electron hopping diffusion coefficient D_e is

$$D_e = \frac{1}{2\nu t_e}\left[\delta^2 + \nu\lambda^2\left(\frac{\rho}{1+\rho}\right)\right] \qquad (22)$$

The limiting expression when physical motion is much faster than electron hopping is

$$D_e = (\delta^2 + \nu\lambda^2)/(2\nu t_e) \qquad (23)$$

(38) The equations of ref 31b have been reduced to the limit where $\omega \ll \beta$ (notation of ref 31b) in which the time required to diffuse across the potential energy well is much longer than the fundamental period of the corresponding harmonic oscillator.

(39) These simulations employed the same algorithm described in the text and Appendix with the following modifications. Periodic boundary conditions were applied along the x-axis, and the electrode reactions at $x = 1$ and $x = N_x$ were eliminated (all molecules were reduced and no electron hopping occurred). The simulations were run until a steady state was reached, at which time the positions of the molecules were recorded. The simulation was continued with the mean-squared displacement of the molecules output at regular intervals.

(40) (a) Von Smoluchowski, M. *Ann. Phys.* **1915**, *48*, 1103. (b) Von Smoluchowski, *Z. Phys. Chem.* **1917**, *92*, 129. (c) Wilemski, G. *J. Stat. Phys.* **1976**, *14*, 153.

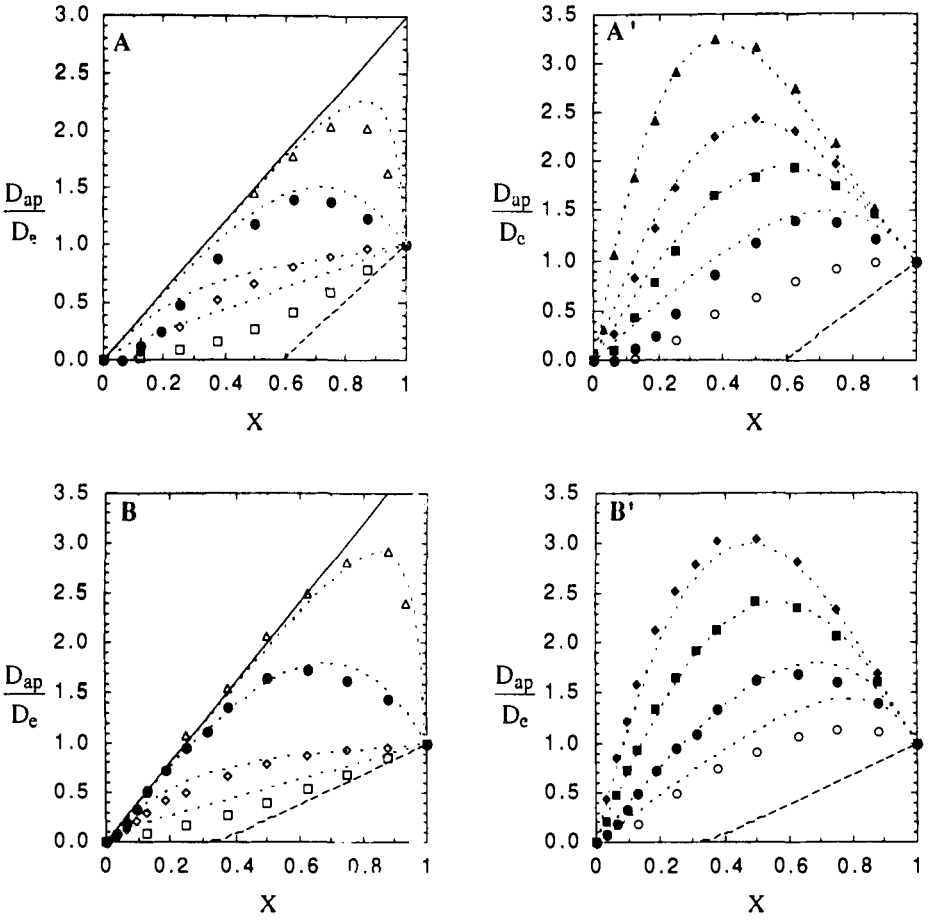

Figure 3. Variation of D_{ap}/D_e with x for square (A, A′) and simple cubic (B, B′) lattices for bounded diffusion. The points in A and B are simulation results for $\lambda/\delta = 1.0$ and $t_e/t_p = 0.1$ (□), 1.0 (◇), 10 (●), and 100 (△). The points in A′ and B′ are simulation results for $\lambda/\delta = 10$ and $t_e/t_p = 0.7$ (○), 1.0 (●), 1.5 (■), 2.0 (◆), and 3.0 (▲, A′ only). The dashed lines represent static percolation behavior (vide supra). The dotted lines represent mean-field behavior (eqs 20–22). The solid lines represent the limiting mean-field behavior for $t_e/t_p \rightarrow \infty$ (eqs 21 and 23).

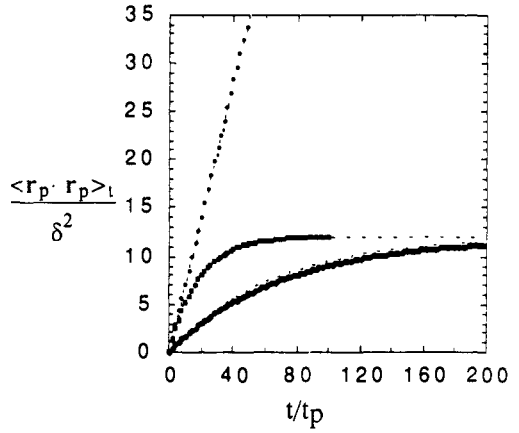

Figure 4. Variation of $\langle \mathbf{r}_p \cdot \mathbf{r}_p \rangle_t/\delta^2$ with t/t_p in a simple cubic lattice. The dashed lines represent the predictions of eqs 13 and 18 with f_c given by eq 17. The points are the results of simulations for $x = 0.25$ and $\lambda \rightarrow \infty$ (◆), $x = 0.25$ and $\lambda = 2\delta$ (■), and $x = 0.75$ and $\lambda = 2\delta$ (●).

Equation 21 with D_e given by eq 23 can be also be derived in the context of Fick's second law by a different method, which is presented in the Appendix. Under conditions where physical diffusion is very rapid, the direct proportionality of D_{ap} with X predicted by Laviron[21a] and by Andrieux and Savéant[21b] is observed. The value of Δx^2 in these derivations is now shown to be equal to $\delta^2 + \nu\lambda^2$ rather than simply δ^2, as would be the case if the Laviron–Andrieux-Savéant behavior were regarded as a limiting case ($D_{phys} = 0$) of Dahms–Ruff behavior. The term $\nu\lambda^2$ accounts for the contributions arising from physical displacement. Although there is no contribution to charge transport from bounded physical diffusion in the absence of electron exchange, the presence of electron exchange makes the bounded physical motion significant. There is a synergy between restricted physical diffusion and electron exchange in that physical motion continuously rearranges the distribution of redox centers, allowing the redox molecules to encounter each other, while electron hopping circumvents the diffusive restrictions imposed by the supramolecular structure, allowing physical motion to contribute to charge transport.

Regardless of the magnitude of t_e/t_p, physical motion becomes increasingly less important as $X \rightarrow 1$, because blocking shuts off physical motion of the redox centers. For fractional loadings near unity, the rate of physical motion is sufficiently small that the distance traversed by a reduced molecule between successive electron hops is very small, sufficiently small that the molecular diffusion can be viewed as unrestricted. In the limit $\rho \rightarrow 0$ ($X \rightarrow 1$), eqs 21 and 22 reduce to $D_{ap} = D_e$.

As emphasized above, eqs 21–23 are mean-field expressions and as such are applicable only when $t_e/t_p \geq 1$ (vide supra). This fact is emphasized in Figure 3 (A and B) where simulated values (points) of D_{ap}/D_e as a function of X are compared with the predictions of eqs 21 and 23 (dashed lines) for $\lambda = \delta$ and various values of t_e/t_p. As is evident from the figure, these equations are only applicable when the rate of physical motion exceeds that of electron hopping. In addition, the range of physical motion, characterized by λ, must be sufficiently large to permit significant encounters between a molecule and its nearest neighbors. This criterion is just barely met by $\lambda = \delta$, as evidenced by the slight negative deviations of the simulated points from the theoretical lines at very small values of X.

The range of the restricted diffusion is predicted to have an important influence on the apparent diffusion coefficient, a prediction that is verified in Figure 3 (A′ and B′), where plots of D_{ap}/D_e vs X are presented for $t_e/t_p = 10$ and various values of

λ/δ. For the simple cubic lattice (Figure 3B′), the agreement between the simulation results and the theoretical predictions is very good (given the uncertainty in the simulation results), with D_{ap} observed to be directly proportional to X at low fractional loadings with a slope given by eq 23. The same behavior is observed for the square lattice when $\lambda/\delta = 3$, but for smaller values of λ/δ a significant negative deviation from theory is observed at low fractional loadings.

The negative deviations in Figure 3A′ for $\lambda/\delta = 1$, 1.5, and 2.0 are consistent with the inability of the molecules to interact readily with their nearest neighbors at low fractional loadings. The harmonic model for bounded diffusion leads to a Gaussian spatial distribution of molecules about their fixed points. For the square lattice, the probability of finding a molecule within 1.7λ of its fixed point is 95%; hence a molecule in two dimensions effectively occupies an area of $3\pi\lambda^2$. Nearest neighbor molecules interact significantly only when their areas of occupancy overlap, which occurs, roughly, when $X > \delta^2/(3\pi\lambda^2)$. Equations 21 and 23 are therefore expected to apply, for $X > 0.01$, only when $\lambda > 3\delta$. The corresponding analysis in three dimensions, where molecules spend 95% of their time within 2λ of their fixed points, indicates that significant intermolecular interactions occur when $X > 3\delta^3/(32\pi\lambda^3)$; thus eqs 21 and 23 apply, for $X > 0.01$, only when $\lambda > 1.4\delta$.

Conclusions

The interdependence between physical displacement and electron hopping in propagating charge through supramolecular redox systems leads to two limiting behaviors: percolation behavior ($k_{diff} < k_{act}$) and mean-field behavior ($k_{diff} > k_{act}$). When physical motion is either nonexistent or much slower than electron hopping, charge propagation is fundamentally a percolation process, because the microscopic distribution of redox centers plays a critical role in dictating the rate of charge transport. Any self-similarity of the molecular clusters between successive electron hops imparts a memory effect making the exact adjacent-site connectivity between the molecules important. In the opposite extreme, rapid molecular motion thoroughly rearranges the molecular distribution between successive electron hops, thereby eliminating an electron's memory of its previous environment. Under such conditions, mean-field behavior is observed.

Theoretical treatments[12,13b-d,21a,b] leading to the Dahms–Ruff or Laviron–Andrieux–Savéant equation are invariably based upon an assumption that is justifiable only under mean-field conditions. These analyses treat the occupancy of each site in a *time-averaged* manner; that is, a specific site is assumed to be occupied a certain percentage of the time. If no electron transfer can occur between two sites at one instant in time, perhaps because one site is unoccupied, electron transfer might nevertheless be possible at a later time, because the site might have become occupied. Under mean-field conditions, the system forgets its state at *all* earlier times. This lack of memory is only possible if the system rearranges rapidly compared to the rate of electron exchange. Utilization of the mean-field approximation therefore presupposes $k_{diff} > k_{act}$.

For this reason, the Dahms–Ruff approach leading to eq 16 (when blocking and correlation effects are taken into account) does not accurately describe charge propagation occurring by means of electron hopping in systems where the redox centers are irreversibly attached to the supramolecular structures and are thereby unable to contribute directly to charge transport through their physical motion. Indeed, when D_{phys} is made smaller and smaller, eventually becoming less than D_e, percolation effects appear. When D_{phys} becomes negligible compared to D_e, the characteristic static percolation behavior ($D_{ap} = 0$ below the percolation threshold and an abrupt onset of conduction at the critical fractional loading) should be observed. In the framework of the present model, it is noteworthy that for freely diffusing redox centers, the fulfilment of mean-field conditions, required for the validity of the Dahms–Ruff equation, implies a descending (or at best horizontal) variation of the apparent diffusion coefficient with the fractional loading and not the commonly expected ascending variation.

The concept of bounded diffusion provides an attractive framework for modeling charge transport occurring via electron hopping in systems where the redox centers are irreversibly attached to the supramolecular structures. Provided the rate of bounded diffusion is much greater than that of electron hopping and the range of bounded diffusion is sufficiently large to allow interactions between neighboring redox centers, the mean-field approximation can be applied. Under these conditions, for fractional loadings commonly employed in practice, the Laviron–Andrieux–Savéant expression (eq 2) predicting the direct proportionality between D_{ap} and X applies. The rate constant appearing in eq 2 is the activation-controlled rate constant for electron exchange and not a combination of diffusion- and activation-controlled rate constants. This does not mean that physical motion is not significant or is not accounted for in eq 2. The rate and range of physical motion must, in fact, be larger than those of electron hopping for the equation to be valid. Moreover, the characteristic mean-squared displacement Δx^2 is not equal to the square of the electron hopping distance, δ^2, but rather to $\delta^2 + \nu\lambda^2$, where λ characterizes the range of physical displacement permitted by the irreversible attachment of the redox centers to the supramolecular structure. The bounded physical motion should be taken into account when attempting to derive the rate constant of electron hopping from experimental values for the apparent diffusion coefficient.

An important simplication employed in this study is the assumption that electron exchange occurs only across a distance δ representing the center-to-center distance of closest approach for the redox molecules. Numerous studies[41] of electron transfer have demonstrated the possibility of long-range electron transfer, with the rate of electron transfer across a distance r being

$$k_{act}(r) = k_{act}(\delta) \exp(-(r - \delta)/\gamma)$$

where the parameter γ characterizes the rate of drop-off in $k_{act}(r)$ with increasing r being typically on the order of 0.07–0.14 nm.[41c] Long-range electron transfer has been suggested to be important in charge transport in supramolecular systems.[25] In the mean-field limit, where the Laviron–Andrieux–Savéant equation applies, long-range electron transport does not appear to be especially significant. Electron transfer over all distances is readily incorporated into the existing theory by employing suitably weighted values for the electron-transfer rate constant and the mean-squared hopping distance. Because $\gamma \ll (\delta^2 + \nu\lambda^2)^{1/2}$, the effects of long-range electron transfer will be small, with k_{act} and δ^2 being replaced, to a first approximation, by $k_{act}(1 - \gamma/\delta)^2$ and $(\delta + \gamma)^2$, respectively. Under conditions where $\lambda \ll \delta$, i.e., when percolation interferes, however, long-range electron transfer may play an important role by providing a mechanism by which an electron can escape from its current cluster without significant rearrangement of the system.

Acknowledgment. D.N.B. was the grateful recipient of a Chateaubriand Fellowship, which was supported in part by Elf Aquitaine. We thank Dr. K.-B. Su for his assistance in the use of the FPS array processor.

Appendix

Simulations. A typical simulation was performed in the following manner. The lattice was constructed and the appropriate number of redox molecules introduced at random lattice sites; for simulations involving restricted diffusion, the molecules were initially located at their fixed sites. All simulations employed boundary conditions in which all molecules at $x = \delta$ were reduced and all molecules at $x = N_x\delta$ were oxidized. The initial oxidation states of the molecules were chosen to produce a linear concentration gradient of reduced molecules (i.e., the steady-state con-

(41) (a) For a review of this field see parts b and c and references cited therein. (b) Chance, B.; DeVault, D.; Frauenfelder, H.; Marcus, R. A.; Schrieffer, J. R.; Sutin, N., Eds. *Tunneling in Biological Systems*; Academic Press: New York, 1979. (c) Mayo, S. L.; Ellis, W. R.; Crutchley, R. J.; Gray, H. B. *Science* **1986**, *233*, 948.

centration profile) in order to reduce the simulation time required to reach a steady state.

Dimensions for square lattices were $N_x = N_y = 32$ ($N_z = 1$) and for simple cubic lattices $N_x = N_y = N_z = 24$, except for static percolation simulations on the square lattice (open circles in Figure 1A) where $N_x = N_y = 64$ and in Figure 3 where $N_x = N_y = N_z = 16$. To increase the effective size of the system, periodic boundary conditions were employed along the xy- and xz-boundaries, so that molecules or electrons jumping, for example, from $y = N_y\delta$ to $y = (N_y + 1)\delta$ were actually moved from $y = N_y\delta$ to $y = \delta$. This technique gave the impression of an infinite system along the y- and z-axes. For restricted diffusion, it was necessary to know the absolute displacement of a molecule from its fixed site. To correctly determine this distance, a record was kept of each passage of a molecule across a lattice boundary in order to permit determination of each molecule's effective position (which may lie far outside the lattice).

Each simulation consisted of a series of time intervals (typically 10^4–10^6) during which the molecules and electrons were allowed to move as described above. The values of $\Delta\tau$ and $(t_e/t_p)\Delta\tau$ were always ≤ 0.25. At the end of each time interval, oxidized molecules reaching $x = \delta$ were reduced and reduced molecules reaching $x = N_x\delta$ were oxidized. The total numbers of electrons introduced and removed from the system during each time interval were averaged and added to the cumulative charge Q_T, which was output periodically. Plots of Q_T versus the simulation time t were examined to determine when a steady state, characterized by a linear increase in Q_T with t, had been reached. The apparent diffusion coefficient was calculated from the measured slope of the steady-state plot Q_T vs t using

$$D_{ap} = \frac{N_x(N_x - 1)\delta^2}{2N_E}\frac{dQ_T}{dt}$$

For free diffusion the steady state was quickly established, generally within tens or hundreds of time intervals. For restricted diffusion, however, very long times ($>10^5$ intervals) were sometimes necessary to achieve the steady state. This problem was most severe for restricted diffusion near full fractional loading (when equilibration of the molecules within the parabolic energy well was very slow) or when t_e/t_p was significantly less than 0.1 or greater than 10.

In order to obtain good statistics, multiple simulations were performed for the same set of parameters (N_x, N_y, N_z, N_E, $\Delta\tau$, $(t_e/t_p)\Delta\tau$, and λ/δ) using different sets of random numbers, and the resulting values of D_{ap} were averaged. This procedure was especially important in cases where the initial distribution of molecules was critical in determining the apparent diffusion coefficients (i.e., static percolation and highly restricted diffusion). Most simulations of D_{ap}/D_e or D_{ap}/D_{phys} were performed to a precision of 2%. Simulations of restricted diffusion with $t_e/t_p = 100$ were especially difficult, and the uncertainty in this data was larger.

Computations were performed using programs written in FORTRAN and executed on a CDC Cyber 962 computer or on an FPS M64330 array processor attached to a DEC VAX station II/GPX. Simulation times for computing a single value of D_{ap} varied from several minutes to several hours, depending upon the choice of parameters and the desired precision.

A few of our simulations duplicated previously published work, specifically, the 2D and 3D static percolation plots[26b,c] (open circles in Figure 2), the 2D dynamic percolation plot[27a] for $t_e/t_p = 0.01$ (solid triangles in Figure 2A), and the plots for physical diffusion in the absence of electron hopping for the simple cubic lattice[36b,37f] (× in Figure 2B′). In all cases, our simulations yielded values in excellent agreement with the published results.

Derivation of $I(\phi/\lambda)$. In a system where the molecules are in thermal equilibrium, the Boltzmann distribution,

$$p(x,x_0) = p_0 \exp\left(-\left(\frac{x - x_0}{\lambda}\right)^2\right)$$

can be employed to determine the probability $p(x,x_0)$ of finding a molecule with fixed point x_0 at position x. For a one-dimensional system in which x lies within the interval $[0,\phi]$, the normalization constant p_0 is

$$p_0 = \left(\frac{2}{\lambda\pi^{1/2}}\right)\Big/\left[\operatorname{erf}\left(\frac{\phi - x_0}{\lambda}\right) + \operatorname{erf}\left(\frac{x_0}{\lambda}\right)\right]$$

The steady-state behavior of a diffusing, reduced molecule in a potential energy well is described by the general diffusion equation[40]

$$0 = D_{ap,\phi/\lambda=0}\frac{\partial}{\partial x}\left[\frac{\partial p_B(x,x_0)}{\partial x} + \frac{p_B(x,x_0)}{k_BT}\frac{\partial \epsilon(x,x_0)}{\partial x}\right] \quad (24)$$

where $p_B(x,x_0)$ is the probability of finding a reduced molecule with fixed point x_0 at position x and the molecule's potential energy, $\epsilon(x,x_0)$, is defined by eq 7. We define $b(x,x_0)$ to be the probability that a molecule with fixed point x_0 found at position x is reduced; thus

$$p_B(x,x_0) = p(x,x_0)\ b(x,x_0)$$

Substitution of the expressions for p_B and $\epsilon(x,x_0)$ into eq 24 yields

$$0 = \frac{\partial^2 b(x,x_0)}{\partial x^2} - \frac{2}{\lambda^2}(x - x_0)\frac{\partial b(x,x_0)}{\partial x}$$

the solution of which, obtained by explicit integration, is

$$b(x,x_0) = \left(\frac{\partial b(x,x_0}{\partial x}\right)_{x=0}\int_{x=0}^{x}\exp\left(\left(\frac{\alpha - x_0}{\lambda}\right)^2\right)d\alpha = b(0,x_0)$$

If the concentration, C_E, of fixed points is uniform throughout the system, the concentration, $C_B(x)$, of reduced molecules at position x is

$$C_B(x) = C_E\int_0^\phi p_B(x,x_0)\,dx_0 = C_E\int_0^\phi p(x,x_0)\ b(x,x_0)\,dx_0 \quad (25)$$

The probability that a molecule at $x = 0$ or $x = \phi$ is reduced is independent of the molecule's fixed point; therefore the mean concentration gradient across the system is

$$\left(\frac{\partial C_B(x)}{\partial x}\right)_{mean} = \frac{C_B(\phi) - C_B(0)}{\phi} = C_E\frac{b(\phi) - b(0)}{\phi} = \frac{C_E}{\phi}\left(\frac{\partial b(x,x_0)}{\partial x}\right)_{x=0}\int_0^\phi \exp\left(\left(\frac{x - x_0}{\lambda}\right)^2\right)dx$$

The steady-state flux of B (and hence of electrons), J_e, across the system

$$J_e = D_{ap,\phi/\lambda=0}C_E\int_0^\phi\left[\frac{\partial p_B}{\partial x} + \frac{P_B}{k_BT}\frac{\partial \epsilon}{\partial x}\right]dx_0 = D_{ap,\phi/\lambda=0}C_E\int_0^\phi p(x,x_0)\frac{\partial b(x,x_0)}{\partial x}\,dx_0 \quad (26)$$

must be the same at all points. Evaluating eqs 25 and 26 at $x = 0$ and substituting these expressions into eq 10 yield

$$D_{ap} = D_{ap,\phi/\lambda=0}\frac{C_E}{(\partial C_B/\partial x)_{mean}}\int_0^\phi p(0,x_0)\left(\frac{\partial b(x,x_0)}{\partial x}\right)_{x=0}dx_0 = D_{ap,\phi/\lambda=0}I(\phi/\lambda)$$

where $I(\phi/\lambda)$ is defined by

$$I(\phi/\lambda) = \frac{2}{\pi^{1/2}}\left(\frac{\phi}{\lambda}\right)\int_0^{\phi/\lambda}\left[(\operatorname{erf}(\phi - \alpha) + \operatorname{erf}(\alpha))\int_0^{\phi/\lambda}\exp((\beta - \alpha)^2)\,d\beta\right]^{-1}d\alpha \quad (27)$$

Derivation of Fick's Second Law for Restricted Diffusion. We derive Fick's second law for a one-dimensional system of infinite

size in which the rate of molecular motion is sufficiently fast to maintain thermal equilibrium at all times; the normalization constant for the Boltzmann distribution is $p_0 = 1/(\lambda\pi^{1/2})$ for x on $(-\infty,+\infty)$. The concentration of reduced molecules B at point x at time t is given by an expression analogous to eq 25, which when integrated over all x_0, with $b(x_0,t)$ expanded as a Taylor series about $x = x_0$, yields

$$C_B(x,t) = C_E\int_{-\infty}^{+\infty} b(x_0,t)\, p(x,x_0)\, dx_0 = C_E\sum_{n=0}^{\infty}\frac{1}{n!}\left(\frac{\lambda}{2}\right)^{2n}\left(\frac{\partial^{2n}b(x,t)}{\partial x^{2n}}\right)_x \approx C_E b(x,t) \quad (28)$$

Note that the function $b(x,x_0)$ defined in the preceding section is independent of the molecule's position for a system of infinite size but does dependent upon time for non-steady-state conditions; hence we write $b(x_0,t)$ instead of $b(x,x_0)$. Truncation of eq 28 after the first term introduces negligible error so long as the thickness of the diffusion layer is much larger than λ. Therefore, Fick's second law

$$\frac{\partial C_B(x,t)}{\partial t} = D_{ap}\frac{\partial^2 C_B(x,t)}{\partial x^2}$$

is completely equivalent to

$$\frac{\partial b(x,t)}{\partial t} = D_{ap}\frac{\partial^2 b(x,t)}{\partial x^2} \quad (29)$$

Because the molecules are always at thermal equilibrium within the potential energy well, there is no net transport of charge arising from physical motion. The time dependence of $b(x,t)$ arises exclusively from electron hopping; hence we apply the standard rate laws to evaluate the rate of change in $b(x,t)$ arising from electron exchange reactions. To account for all electron-transfer reactions affecting $b(x_0,t)$, we must locate all molecules possessing fixed point x_0, their current positions being x, and all molecules of the opposite oxidation state within a distance δ of x, such molecules having fixed points at $\hat{x}_0$. The rate constant for electron exchange between two *specific* molecules is k_{act} divided by the reaction surface "area" (recall that k_{act} applies to electron transfer to *any* site within the reaction distance δ). In one dimension this quantity is $k_{act}/2$, in two dimensions $k_{act}/(2\pi\delta)$, and in three dimensions $k_{act}/(4\pi\delta^2)$. The resulting master kinetic equation in one dimension is

$$\frac{\partial b(x_0,t)}{\partial t} = \frac{k_{act}C_E}{2\lambda^2\pi}\int_{-\infty}^{+\infty}\int_{-\infty}^{+\infty}(b(\hat{x}_0,t) - b(x_0,t))p(x,x_0) \times (p(x-\delta,\hat{x}_0) + p(x+\delta,\hat{x}_0))\, dx\, d\hat{x}_0$$

Expansion of $b(\hat{x}_0,t)$ as a Taylor series about x_0 followed by integration over $\hat{x}_0$ and x, using binomial series expansions where necessary, yields

$$\frac{\partial b(x_0,t)}{\partial t} = k_{act}C_E\sum_{n=1}^{\infty}\left(\frac{\partial^{2n}b(x,t)}{\partial x^{2n}}\right)_{x_0}\sum_{m=0}^{n}\sum_{k=m}^{n}\frac{(\lambda/2)^{2k}\delta^{2n-2k}}{(k-m)!\,(2n-2k)!} \quad (30)$$

The derivations in two and three dimensions are completely analogous to that shown above, except that the reaction surface is a circle in two dimensions and a sphere in three dimensions; the exact expressions for $\partial b(x_0,t)/\partial t$ in two and three dimensions are, of course, slightly different than that of eq 30. Provided the diffusion layer is much larger than λ, only the first term in the series expansion for $\partial b(x_0,t)/\partial t$ is significant. On the basis of the derivations for $\nu = 1$, 2, and 3, with terms for $n \geq 2$ discarded, a general equation is obtained

$$\frac{\partial b(x_0,t)}{\partial t} = \frac{1}{2\nu}k_{act}C_E(\delta^2 + \nu\lambda^2)\left(\frac{\partial^2 b(x,t)}{\partial x^2}\right)_{x_0}$$

which is identical to eq 29 with D_{ap} given by eqs 20 and 22 (written using $k_{act}C_E$ instead of X/t_e).

Identification of the Iron Ions of High Potential Iron Protein from *Chromatium vinosum* within the Protein Frame through Two-Dimensional NMR Experiments

Ivano Bertini,*,† Francesco Capozzi,‡ Stefano Ciurli,‡ Claudio Luchinat,‡ Luigi Messori,† and Mario Piccioli†

Contribution from the Department of Chemistry, University of Florence, Florence, Italy, and the Institute of Agricultural Chemistry, University of Bologna, Bologna, Italy.
Received August 26, 1991

Abstract: 2D NMR experiments performed on both the oxidized and reduced form of the high potential iron protein (HiPIP) from *Chromatium vinosum*, a paramagnetic iron sulfur protein for which the crystal structure is known in both oxidation states, allowed us to detect a number of scalar and dipolar connectivities of the isotropically shifted signals. On this basis it was possible to firmly identify the signals of the β-CH_2 and α-CH protons of the cluster-liganded cysteines and perform their sequence-specific assignments. The assignments mainly rely on the observation of NOESY cross peaks from β or α Cys protons to protons assigned to the few aromatic residues surrounding the cluster. This is the first sequence-specific assignment of Cys β-CH_2 protons for a Fe_4S_4 cluster. In the light of existing experimental evidence from Mössbauer data and of the theoretical model describing the magnetic coupling of the metal centers in the oxidized form, the present assignment establishes which iron ions of the oxidized cluster are in a pure ferric state and which are in a mixed valence state. These findings may be relevant as far as the actual mechanism of electron transfer is concerned. In addition, information is obtained on the angular dependence of the β-CH_2 hyperfine shifts in iron sulfur systems.

Introduction

The understanding of the functional properties of iron–sulfur proteins[1] stands on the knowledge of the electronic structure of the clusters and on the location of the various types of iron ions within the protein frame. Progress in the knowledge of the electronic structure of iron–sulfur clusters is due to a variety of

† University of Florence.
‡ University of Bologna.

(1) (a) Lovenberg, W., Ed. *Iron Sulfur Proteins*; Academic Press: New York, 1973, Vol. 1, 2; 1977, Vol. 3. (b) Spiro, T. G., Ed. *Metal Ions in Biology*; Wiley-Interscience: New York, 1982; Vol. 4. (c) Sweeney, W. V.; Rabinowitz, J. C. *Annu. Rev. Biochem.* **1980**, *49*, 139.

0002-7863/92/1514-3332$03.00/0